Coarse-scale Modeling of Flow in Gas-injection Processes for Enhanced Oil Recovery

Verity Borthwick, Farid Bozorgnia, Francesco Cadinu, Henrik Holst,
Mohammad Motamed, Fritjof Nilsson, Jelena Popovic

June 29, 2007

1 Introduction

The numerical simulation of oil recovery by gas injection presents significant challenges. The governing dimensionless pressure equation is obtained by combining the continuity equation $\nabla \cdot \mathbf{u} = \mathbf{0}$ and Darcy's law given by $\mathbf{u} = -\mathbf{k} \cdot \nabla p$, which leads to

$$\nabla \cdot (\mathbf{k} \cdot \nabla p) = 0. \tag{1}$$

In solving the pressure equation (1), we must deal with extreme heterogeneity in the permeability field, which varies over several orders of magnitude and exhibits sharp contrasts due to geological features such as channels or faults. Unfortunately, because both the spatial and temporal domains for these problems are quite large, computing solutions on a fine scale is not practical, thus requiring upscaling of the permeability field, or the associated transmissibility, to a much coarser scale. However, straightforward upscaling techniques are not effective for these problems, because they cause smoothing of fine-scale effects that significantly affect the estimation of essential quantities that measure the effectiveness of gas-injection processes, such as global sweep efficiency and breakthrough time. In this report, we will modify newly developed upscaling methods for resolving these difficulties. The modifications will give both accuracy and efficiency improvements.

2 Upscaling Methods

2.1 Multi-Level Local-Global Method (MLLG)

In local-global methods [1], the advantages of both approaches (local and global) are used. Local methods use generic fine-scale flows on a local region centered around the face to compute the upscaled transmissibility for a coarse grid face. These methods are attractive because of their low computational cost and ease of implementation. Although they may give satisfactory results for some permeability fields, they in general do not perform well on reservoirs with important large-scale connected flow paths, or if flow is not aligned with the grid [5]. Global methods [4] are developed as a tool to improve the accuracy of local methods. They use global or approximate global fine scale flow simulations to determine coarse scale parameters and in that way reduce the error due to connected flow path. The main disadvantage is that these methods are computationally expensive. In local-global methods, the local approach is first used to find a coarse permeability or transmissibility field. Next, the pressure is computed on the coarse grid with generic boundary conditions. The coarse solution is interpolated to obtain new boundary values for the local regions. The process is repeated until the convergence of the coarse field. The basic idea behind MLLG is to combine the local-global approach with grid adaptivity [3].

2.2 Variable Compact Multi-Point Method (VCMP)

In cases with strong full tensor anisotropy, multi-point flux approximations (MPFA) have been found to be more accurate than the more robust two-point flux approximations (TPFA). It will then be desirable to construct an algorithm based on the local MPFA remaining as close to a TPFA as possible in the case

of an isotropic permeability field. VCMP uses a weighted MPFA to honor this property. Like in MLLG, an adaptive grid is also used in VCMP. However, the algorithm is not based on iterations to achieve consistency between local and global solutions. See [5] for more details.

2.3 Hybrid Method VCMP / MLLG

The hybrid method combines VCMP and MLLG in order to improve the performance of both methods. The algorithm is based on VCMP and benefits from the iterative procedure in MLLG combined with Dirichlet conditions for local solves.

2.3.1 Interpolation

The hybrid method uses first-order interpolation to obtain boundary conditions for extended local regions (local region extended with neighbouring coarse regions). The method can be improved by performing higher order interpolation. However, the interpolant may exhibit oscillatory behavior. It is therefore advisable to use high-order Essentially Non-Oscillatory (ENO) interpolation in order to maintain the monotonicity in the pressure field.

In this project, we modified the algorithm by using three different interpolation schemes: cubic spline interpolation (Hybrid 1), quadratic interpolation (Hybrid 2) and the combination of the two (Hybrid 3). We perform different upscaling methods on three different permeability fields which are taken from [2] and shown in Figure 1.

The maximum error in velocity field for different permeability fields is shown in Table 1.

	Maximum error					
Model	MLLG	VCMP	Hybrid (linear interpolation)	Hybrid 1 (cubic spline)	Hybrid 2 (quadratic spline)	Hybrid 3 (cubic and quadratic)
1	0.333	0.112	0.135	0.069	0.101	0.071
2	0.114	0.106	0.044	0.085	0.079	0.048
3	0.051	0.056	0.054	0.053	0.061	0.051

Table 1: Maximum error in velocity field for 3 different models obtained by different upscaling methods. Hybrid 1,2 and 3 represent the modified Hybrid method using different interpolation schemes.

As it can be seen from Table 1, interpolation plays an important role in the performance of the numerical algorithm. In Models 1 and 3 we have obtained 50% and 6% improvement in the error, respectively.

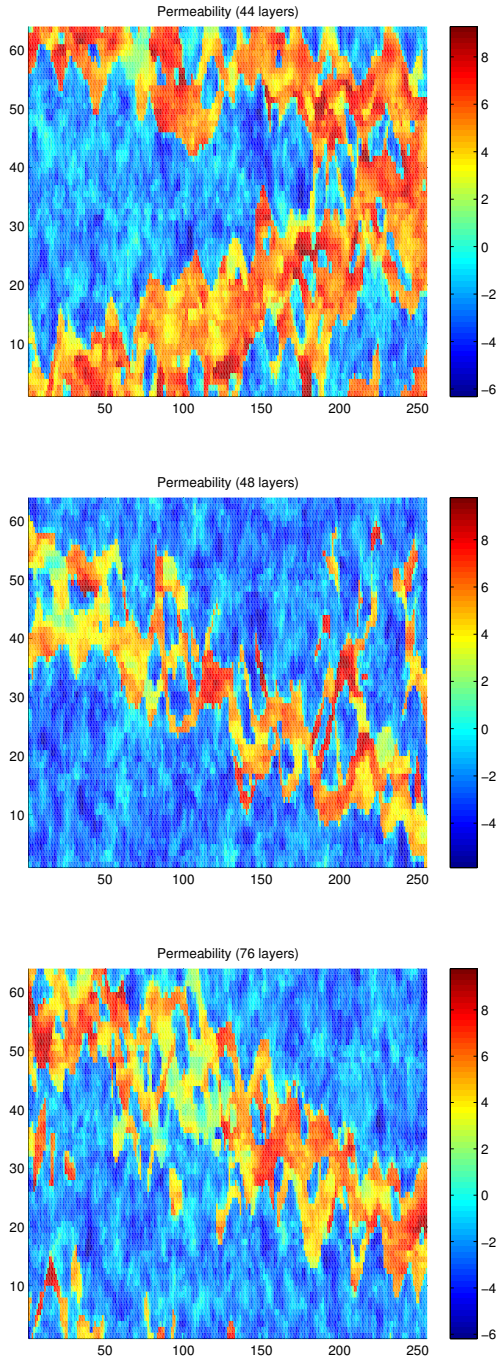

Figure 1: The permeability fields of three different models.

3 Flow based adaptivity criteria

We will propose a method to reduce the amount of refinement necessary to resolve the flow in channels which are aligned with the grid. The current code

refines the grid when the flow q_i over a face is larger than some specified threshold. The threshold is given by the expression,

$$|q_i| > \alpha \left(\frac{A_i}{A} \right) \frac{A_i}{A} |Q| \tag{2}$$

and the α function should be approximately equal to the parameter $\delta \geq 1$ on the coarsest grid and α should be equal to $\frac{A}{A_i}$ on the finest grid. Increasing δ will give less refinement. As an example, if $\delta = 1$ then we have the condition $|q_i| > \frac{A_i}{A}|Q|$ on the coarsest grid, which is equivalent to

$$\frac{|q_i|}{A_i} > \frac{|Q|}{A}.$$

This means that we refine if the average velocity over the face i is larger than the global average velocity. On the finest grid, the condition becomes

$$|q_i| > |Q|$$

which means that the flow over face i is *larger* than the total flow, which is absurd. Hence no further refinement will occur.

Since every refinement increases the complexity of the grid, we want to achieve a greater efficiency by decreasing the number of refinements, without compromising the overall accuracy of the results. The basic idea is to detect the faces (cells) where the flow is aligned with the grid (i.e. is along the x-axis) and don't flag them for refinement even the condition (2) is met.

To simplify the exposition, assume that the face i is perpendicular to the x-direction. If we refer to the two cells separated by the face i as "source" and "target" cells, we can describe the criteria as follows:

1. Incoming flow into the source cell must be approximately equal to the outgoing flow from the source cell. The flow is measured in the x direction.

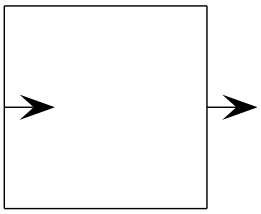

Face flow condition 1.

2. The outgoing flow in the x direction from the target cells (one or two) must be approximately equal to the outgoing flow from the source cell.

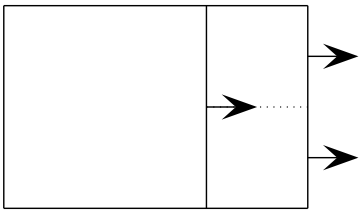

Face flow condition 2.

3. The flow in the y direction must be negligible with respect to the flow in the x direction.

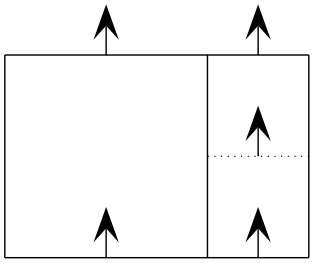

Face flow condition 3.

4 Anisotropic Refinement

For efficient adaptive simulation of reservoir systems, a grid topology should ideally facilitate a fast transition from fine to coarse scales. A Cartesian-based grid with anistropic refinement has been applied to the test data, Model 1. This grid is formed by making a number of refinements of the cells by splitting them if deemed necessary by the flow adaptivity criteria. While anisotropic refinement significantly reduces the amount of cells, it introduces a large amount of error. The aim is to try and reduce number of cells and error by introducing changes into the anisotropic refinement procedure.

Four different methods of anisotropic refinement were applied to Model 1. The aim of this was to test which gave the best result with regard to reduction of percentage error of global flow (GF) and the number of cells. It was also important to maintain a good match between the fine scale data and the coarse scale data, and preserve the flow information.

The simulation was first run for isotropic refinement only, to provide a comparison for the further methods applied. First, normal anisotropic refinement (method one) was applied with no modifications. Whenever a face is flagged for refinement based on the adaptivity criteria, it is only performed along one dimension, where the choice of dimension is dependent on the reason for flagging. The next step was to reduce the anisotropy so it was selectively applied (method two). In effect, this meant refining isotropically over the important cells, i.e., cells in a high flow area, while refining anisotropically over the remaining cells. We then experimented with limiting the aspect ratio (method three) since in some cells this was very large, for example 1:8. Large aspect ratios increase the truncation error in the discretization of the pressure equation, and thus removing them may have a beneficial effect. The code was changed to restrict the aspect ratio to 1:4 to try to avoid this problem. The final change we applied to the anisotropic refinement was applied to the previous refinement (method three i.e., that with the limited aspect ratio). Further selective refinement was applied to important cells, the cells in high flow regions (method four). The results from each method were compared to the isotropic grid and also to the other anisotropic methods.

5 Numerical results

5.1 Hybrid MLLG / VCMP Upscaling

The velocity fields obtained by the algorithm giving the minimum error are shown in the following figures for the three described models.

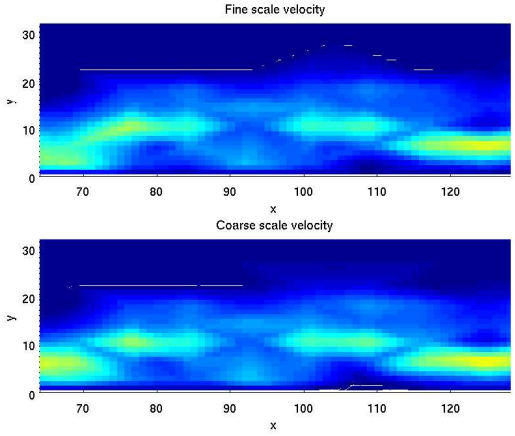

Figure 2: The velocity field in x-direction obtained by the Hybrid 1 method.

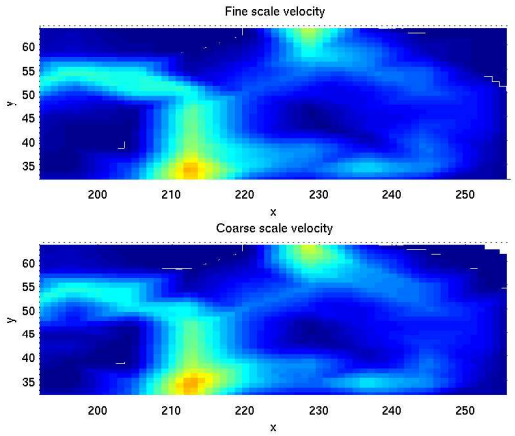

Figure 3: The velocity field in y-direction obtained by the Hybrid 1 method.

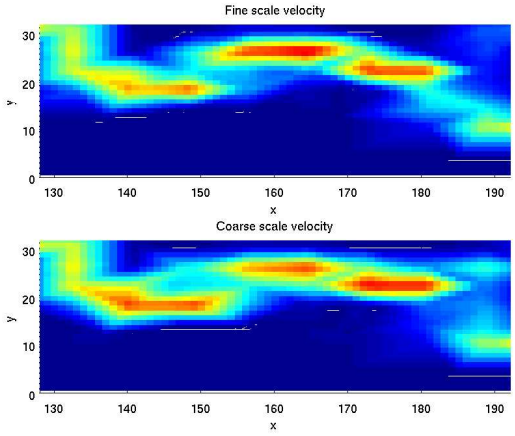

Figure 4: The velocity field in x-direction obtained by the Hybrid 2 method.

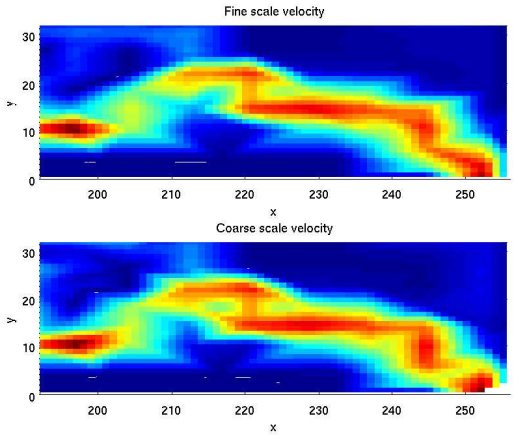

Figure 5: The velocity field in y-direction obtained by the Hybrid 2 method.

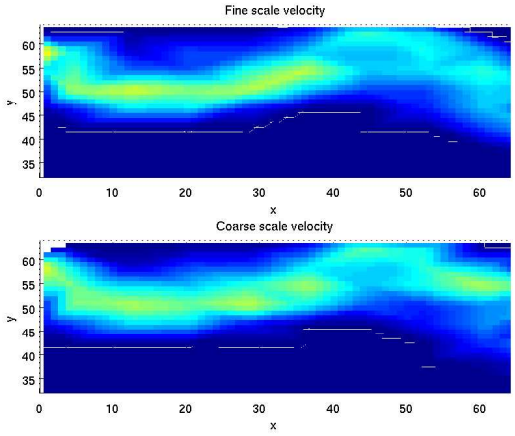

Figure 6: The velocity field in x-direction obtained by the Hybrid 3 method.

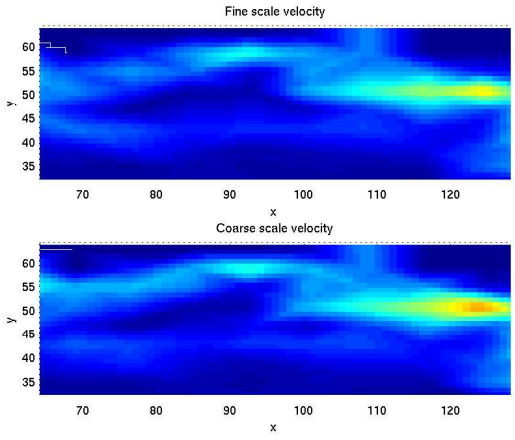

Figure 7: The velocity field in y-direction obtained by the Hybrid 3 method.

5.2 Flow based adaptivity criteria

We wish to test our scheme on two different types of problems. A first case with well-defined channel flow paths, and a second one without channelized flow paths. The permeability field 44 (2.3.1) is chosen as a typical channelized flow case. For the second case, without well-defined channelized flow, we chose permeability field 31 (see Figure 5.2). In the latter case we don't expect our scheme to produce any substantial modifications of the results.

	Original	Modified
No. cells	404	374 (92.5%)
y-dir. flow error	2.59%	2.57%

Table 2: Layer 44, with channel flows

	Original	Modified
No. cells	419	413 (98.6%)
y-dir. flow error	0.76%	0.75%

Table 3: Layer 31, without well-defined channel flows.

We saw about 10% fewer grid cells using our channelized flow detection scheme. We measure the total flow across the domain by measuring the flow at the right boundary and compared it to the left boundary. We saw that our grid gave approximately the same results as the original method, without sacrificing any precision in the total flow. As we can see in Table 2, it works well for this case with well-defined channelized flow. The scheme also works well for the case without well-defined channel flow paths since it naturally disables itself then. This is shown in Table 3.

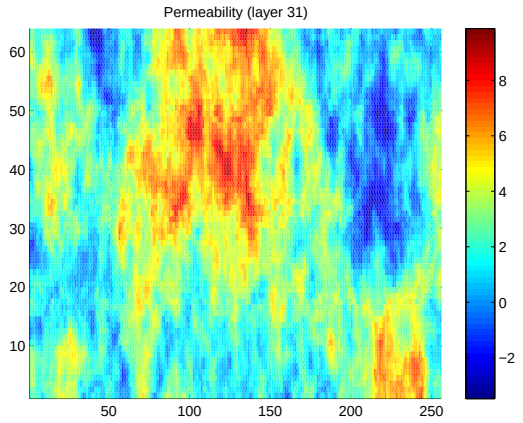

Figure 8: Permeability field for layer 31, without well-defined channels.

5.3 Anisotropic Refinement

The various methods of refinement were compared to both the isotropic refinement (Figure 9) and each other. Table 4 shows a comparison of the results from each of the methods applied.

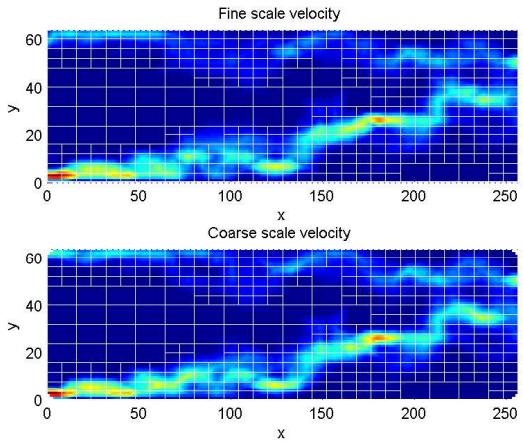

Figure 9: Velocity field from isotropic refinement with grid overlay.

Method	Isotropic	One	Two	Three	Four
No. cells	404	296	400	308	391
x-direction flow (GF)	0.14	0.29	0.13	0.31	0.12
y-direction flow (GF)	0.026	0.14	0.026	0.13	0.027

Table 4: Comparison of different methods.

When normal anisotropic refinement (method one) was applied to the grid, it was seen that in comparison to isotropic refinement while the number of cells decreased significantly, the percentage error in the global flow (GF) in both the x and y directions increased drastically. Figure 10 shows that the coarse scale velocity field does not match the fine scale as well as with isotropic refinement of the grid (Figure 9).

Method two reduced the GF to similar values as the isotropic refinement and the coarse scale velocity field matched well with the fine scale (see Figure 11) but only reduced the grid by four cells.

Application of Method three failed to improve on the original anisotropic refinement. The number of cells was reduced, but not as significantly and the GFs were comparable. Figure 12 shows that the coarse scale velocity field did not match well with the fine scale data. This was the worst of the various methods trialled.

Method four was the most effective of the anisotropic refinement styles trialled. The GF was reduced to similar values as the isotropic but with a reduction

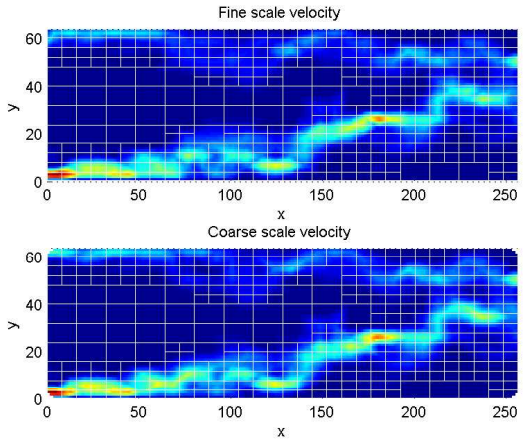

Figure 10: Velocity field from Method One with grid overlay.

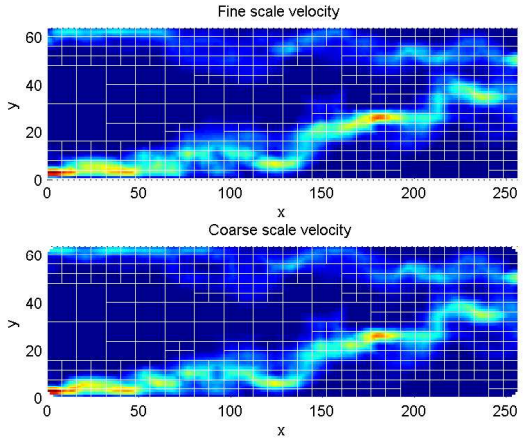

Figure 11: Velocity field from Method Two with grid overlay.

of the grid by 13 cells. Figure Figure 13 shows the coarse scale velocity field matched the fine scale slightly better than the isotropic refinement (Figure 9).

6 Conclusion

We have presented and compared different upscaling algorithms for different permeability models. The recently proposed hybrid method combines multi-level local-global method and variable compact multi-point method. However, in some cases it does not improve the accuracy obtained by the two individual methods. We modified the hybrid method by using higher-order interpolation to obtain the boundary conditions for the extended local regions. The promising results show that interpolation plays an important role in the accuracy of the

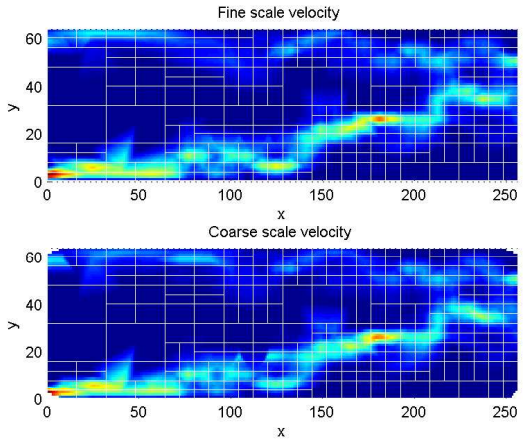

Figure 12: Velocity field from Method Three with grid overlay.

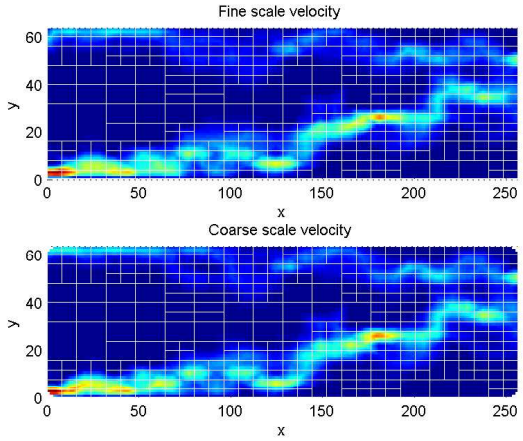

Figure 13: Velocity field for Method Four with grid overlay.

solution. Because of nonphysical oscillations introduced by higher order interpolation, we anticipate that essentially non-oscillatory (ENO) interpolation will further improve the performance of the algorithm.

We have constructed a scheme that detects channel flows parallel to the grid axises, and enable us to reduce the amount of necessary refinement. The numerical tests have shown that our scheme works and succeeds in finding channelized flow paths. Also, the scheme has an equivalent accuracy compared to the original refinement scheme.

From the anisotropic refinement styles applied to Model 1, limiting the aspect ratio coupled with a further refinement over the areas of high flow showed a significant decrease in the amount of cells in the grid, while retaining similar GF errors to the isotropic refinement. The coarse scale velocity field was very similar

to the fine scale velocity field. Due to time constraints we were unable to test the fourth method without limiting the aspect ratio. This may be interesting for further studies to determine whether the effect this procedure has is actually significant. Further research should also include trialling other test layers to see if they behave differently, particularly those which have flow paths that are not aligned with the grid.

References

[1] Y. Chen, L.J. Durlofsky, M. Gerritsen, and X.H. Wen. A coupled local-global upscaling approasch for simulating flow in highly heterogeneous formations. *Advances in Water Resources*, 26:1041–1060, 2003.

[2] M.A. Christie and M.J. Blunt. A comparison of upscaling techniques. *SPE Reservoir Evaluat Eng*, 4:308–317, 2001.

[3] M.G. Gerritsen and J.V. Lambers. A specialized upscaling method for adaptive grids: tight integration of local-global upscaling and adaptivity leads to accurate solution of flow in heterogeneous formations. *Computational Geosciences*, in review, 2007.

[4] L. Holden and B.F. Nielsen. Global upscaling of permeability in heterogeneous reservoirs: the output least squares (OTL) method. *Transport in Porous Media*, 40:115–43, 2000.

[5] J.V. Lambers, M.G. Gerritsen, and B.T. Mallison. Accurate local upscaling with variable compact multi-point transmissibility calculations. *Computational Geosciences*, to appear, 2007.